



Experimental and theoretical investigation of thermoacoustic oscillations in natural gas metering stations

A. Brümmer^{a,*}, R. Edlerherr^a, J. Lenz^b

^a Chair of Fluidics, Faculty of Mechanical Engineering, Technische Universität Dortmund, Leonhard-Euler-Straße 5, 44227 Dortmund, Germany

^b KÖTTER Consulting Engineers KG, Bonifatiusstraße 400, 48432 Rheine, Germany

ARTICLE INFO

Keywords:

Thermoacoustic oscillations
Method of characteristics
Pipe vibration
Flow metering faults
Heat exchanger
Rijke tube oscillation

ABSTRACT

In natural gas flow metering and pressure regulation stations flowmeters, heat exchangers and control valves are usually connected in series. Especially in the case of two or more measuring bars sometimes at minor flow rates untypical pipe vibration together with flow metering faults are observed. Based on field investigations the dependencies between the pipe vibration level, the gas pulsation inside the pipe and the operating conditions of the heat exchanger are analysed. It turns out that with increasing heat flow rates into the natural gas the pulsation and hence the metering faults as well as the pipe vibrations are amplified.

In order to understand the physical dependencies of this phenomenon besides experiment a theoretical study is performed. The origin of the vibration turns out to be a thermoacoustic instability. According to the Rayleigh criterion gas pulsations are amplified if heat is given to the gas at the moment of greatest condensation. Based on detailed theoretical investigations by means of the method of characteristics using a Rijke tube model the physical dependencies are analysed. Finally potential solutions to avoid this vibration problem at natural gas metering stations are introduced.

© 2011 Elsevier Ltd. All rights reserved.

1. Introduction and problem description

Occasionally, pipe vibrations are detected in natural gas pressure regulation and metering stations, which operators can perceive both visually, as structural vibrations at pipes and assemblies, and acoustically. Such vibrations occur, in particular, in stations with at least two adjoining regulating lines with heat exchangers, with a small volume flow flowing through one line and with the other line being unused. In addition, the concurrently arising volume flow pulsation can influence the measuring behaviour of the upstream flowmeters. This problem will be shown more precisely on the basis of a surveyed gas pressure regulation and metering station. Fig. 1 aims to give an overview of the pipe routing (nominal pipe sizes 250/300 mm) with different measuring points for simultaneous recording of the vibration and pressure pulsation situation of the studied natural gas pressure regulation and metering station. Starting from the high-pressure side, the natural gas (operating pressure 4, 7 MPa at 10 °C) flows first through the filter separator (FS) and then through the gas flowmeter with the vortex flowmeter (VFM) being connected in series with the turbine flowmeter (TFM). Afterwards,

operating and stand-by lines with heat exchangers (HE), safety valves (SV) and pressure regulators (PR) towards the low-pressure side follow. In certain operating ranges, structural vibrations and significant deviations in the measuring behaviour of the vortex gas meter and turbine flowmeter occurred in the station.

Based on detailed experimental investigations it turns out that a direct interrelation can be established between the operating conditions of the heat exchanger, such as for example the water temperature, and the intensity of the pulsations inside the natural gas. The results of this investigation and the dependencies of the quantities are presented below.

1.1. Vibration measurements in the station

Apart from the operating parameters, pressure pulsations (e.g. P11abs_A and P6abs_R) and structural vibrations (e.g. S9_U) were simultaneously measured at different measuring points (Fig. 1). In general the vibration phenomenon occurred exclusively at small flow rates and operating heat exchangers. No vibrations were observed in the case of a closed water cycle of the heat exchangers (Fig. 2 before 520 s). The vibrations were excited, in particular, when the water cycle of the heat exchangers was suddenly changed over from the closed (no water through the heat exchanger before 520 s) to the fully open state (maximum water flow rate through the heat exchanger after 520 s). After a short

* Corresponding author. Tel.: +49 231 755 5720; fax: +49 231 755 5722.
E-mail address: andreas.bruemmer@tu-dortmund.de (A. Brümmer).

Abbreviations and formula symbols

c	Flow velocity
c'	Flow velocity pulsation (without mean flow velocity)
d	Inner diameter of Rijke tube
FS	Filter separator
HE	Heat exchanger
l	Rayleigh index
l	Length of Rijke tube
Nu	Nusselt number
p	Time dependent pressure
p'	Pressure pulsation (without mean pressure)
\hat{p}_0	Pressure pulsation amplitude of superposed initial disturbance
\hat{p}	Final pressure pulsation amplitude
P	Pressure pulsation measurement point
PR	Pressure regulator
q	Heat input
q'	Heat input fluctuation (without mean heat input)
Re	Reynolds number
Re_m	Time averaged Reynolds number
S	Pipe vibration measurement point
SV	Safety valves/shut-off valve
t	Time
T	Time period, temperature
TFM	Turbine flow meter
VFM	Vortex flow meter
$\Delta\varphi_{c,q}$	Phase shift between flow velocity pulsation and heat input pulsation (heat input lags flow velocity in the case of $\Delta\varphi_{c,q} > 0$)

delay pressure pulsations with correlating pipe vibrations set in. The highest vibration velocity of the pipe was determined at a flow rate of about $10\,000\text{ N m}^3/\text{h}^1$ (effective vibration velocity of 9 mm/s (rms)). The frequency of the pressure pulsations was about 18 Hz and in phase opposition at the measuring points P6abs_R and P11abs_A. With a distance between both pressure regulators of 11 m and a speed of sound of 400 m/s in the natural gas, this frequency and the measured phase position correspond to the first acoustic natural frequency for pipes acoustically closed at both ends. The experiments showed furthermore that, with rising water temperature and related higher heat input into the gas, the vibrations were amplified.

1.2. Flow-metering faults

Through the gas column, the described pulsations in the area of heat exchangers and pressure regulators interacted also with the turbine flowmeter (TFM) and vortex flowmeter (VFM). Due to the corresponding velocity pulsations metering errors occurred and hence an increased synchronism deviation in the flow-metering devices was initiated. Analogously to the measurements described above, the pressure pulsations in the area of the flow-metering devices were also measured (Fig. 3).

In addition, the vortex shedding frequency of the vortex flowmeter and the HF-impulses of the turbine wheel flowmeter were recorded. The measured values confirm an influence of the volume flow pulsations on the turbine flowmeter and the vortex flowmeter. When pulsations set in, first a failure of the vortex flowmeter occurs. The vortex shedding frequency is no longer proportional to the flow rate. It corresponds to half (9 Hz) of the

pulsation frequency or to the single pulsation frequency (18 Hz) of the pulsations observed. The resulting metering error temporally is above 100% of the true value. In the case of the turbine wheel flowmeter, the spread of the measured flow rates increases directly with the increase in pulsation after the start of the heat exchanger. In parallel a metering error above 10% of the true value may be expected. The spectral analysis of the HF-pulse signal provides a more detailed examination of the influence on the turbine wheel flowmeter. In steady flow without pulsations, the impeller of the turbine wheel flowmeter rotates at constant peripheral speed, which is seen to be in the range between 400 and 520 s in Fig. 4. In the pulsating flow with low to medium pulsation frequency, the peripheral speed of the impeller is pulsating, too. In the colour spectrum of the HF-pulse signal, this frequency modulation is visible through side bands next to the carrier frequency (from 520 s). The distance of the side bands in the frequency axis of the blade pass frequency corresponds to the pulsation frequency of 18 Hz .

2. Analysis of vibration excitation using the example of a Rijke tube

The origin of the phenomenon observed in the station is a thermoacoustic instability between the heat input into the natural gas and the gas-column vibrations inside the pipe. Due to the corresponding pressure and velocity pulsations, the structural vibrations and flow metering errors occur. The following describes the physical mechanism of action of the vibration problem and illustrates its numerical simulation by means of the method of characteristics. Based on the numerical results, the principal dependencies arising in the development of thermoacoustic vibrations are discussed. The Rijke tube is used for this purpose as a simplified model of the station.

2.1. Rijke tube

The Rijke tube is a model experiment which allows the examination of thermoacoustic vibrations. It consists of a horizontally arranged tube with two acoustically open ends where flow is applied from the left to the right side by means of a small blower (Fig. 5). A heat wire which can be positioned at different cross sections in the tube is used as heat source to generate a tonal sound. The frequency of the generated tonal sound corresponds to the first acoustic natural frequency of the tube. Depending on the heat-source position in the tube, the intensity of the tonal sound is amplified or the sound disappears [1].

The criterion developed by Lord Rayleigh in 1878 can be used as a precondition for the development of vibrations: "If heat be given to the air at the moment of greatest condensation, or be taken from it at the moment of greatest rarefaction, the vibration is encouraged. On the other hand, if heat be given at the moment of greatest rarefaction, or abstracted at the moment of greatest condensation, the vibration is discouraged [2]".

This interrelation can be mathematically described by the Rayleigh integral

$$I = \frac{1}{T} \int_t^{t+T} p'(t) \cdot q'(t) dt. \quad (1)$$

Here $p'(t)$ and $q'(t)$ represent the time fluctuations of pressure and heat input, with their product being integrated by a time period T . Depending on the Rayleigh index I ,

$I > 0$ results in an amplification

$I < 0$ results in an attenuation

of an existing disturbance [3].

¹ $\text{N m}^3/\text{h}$ —standard m^3/h at 0°C (273 K), 1013 mbar (0.1013 MPa).

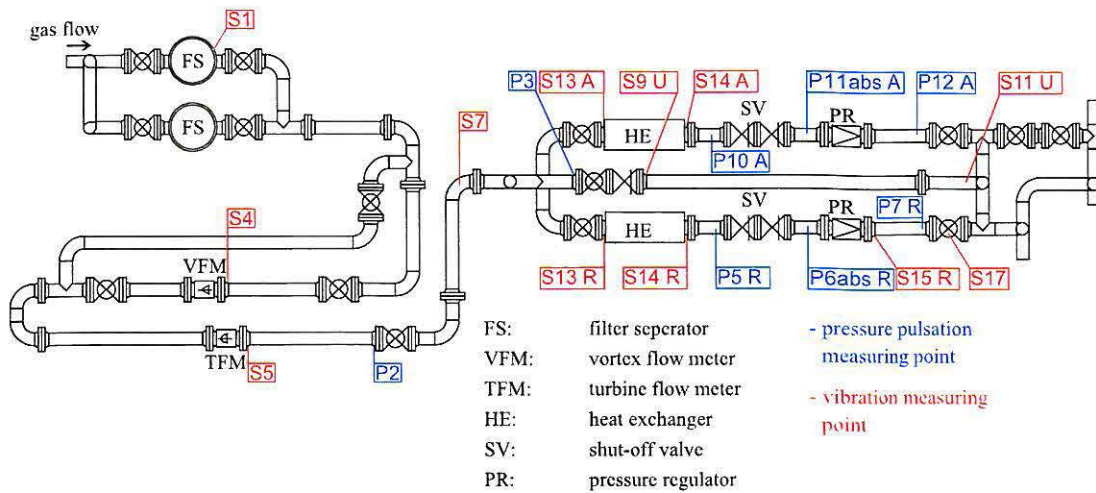


Fig. 1. Overview of the surveyed natural gas pressure regulation and metering station with different measuring points (nominal pipe size 250/300 mm).

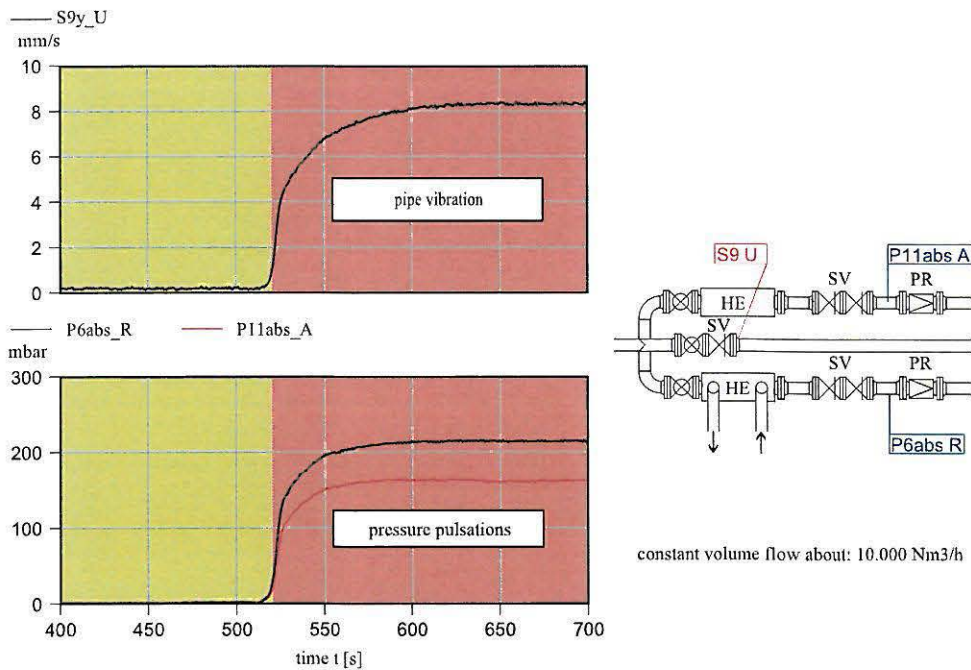


Fig. 2. Pipe vibrations and pressure pulsations before and after suddenly activating the heat exchanger at 520 s (operating pressure inside natural gas 4.7 MPa at 10 °C).

2.2. Numerical modelling of the Rijke tube

For a better understanding of the causes and mechanisms of action in the development of thermoacoustic vibrations, simulations for the Rijke tube according to Fig. 5 were carried out. For this purpose, the Rijke tube is modelled and simulated by means of the one-dimensional method of characteristics [4,5]. Accordingly for calculation of the time-dependent fluid-mechanical values, a system of equations comprising the mass-conservation, the conservation of momentum and the conservation of energy is applied. In order to obtain a solution, the system of hyperbolic partial differential equations is transformed into a system of common differential equations. The solution of the equations is then possible along characteristic curves (eigenvectors of the matrix). With a temporal and spatial discretization as well as the ensuing local linearization of the characteristics, the system of equations is numerically solved [4].

The equivalent numerical model for the Rijke tube has a length of $l = 1$ m and a diameter of $d = 0.06$ m. Dry air is assumed as the fluid. In this simulation, the heat source is located at $l/4$ (Fig. 5). Because of using a one-dimensional method a model is required to reproduce the dependency between the actual local flow velocity and the corresponding heat flow rate into the air. Due to the lack of an easy heat transfer model for pulsating turbulent pipe flows within this investigation the heat transfer model of Michejew and van Leyen described in [6] for steady-state flow is used. According to this model the heat flow rate (Nusselt number) increases with increasing flow velocity (Reynolds number). The mean flow velocity inside the Rijke tube is chosen to be 0.6 m/s flowing from the left to the right side. To account for an always present weak disturbance a sinusoidal pulsation with a fixed frequency and intensity is superposed to the mean velocity. Due to this fluctuating flow velocity the time and space dependent Reynolds number is pulsating too. Therefore the Nusselt number

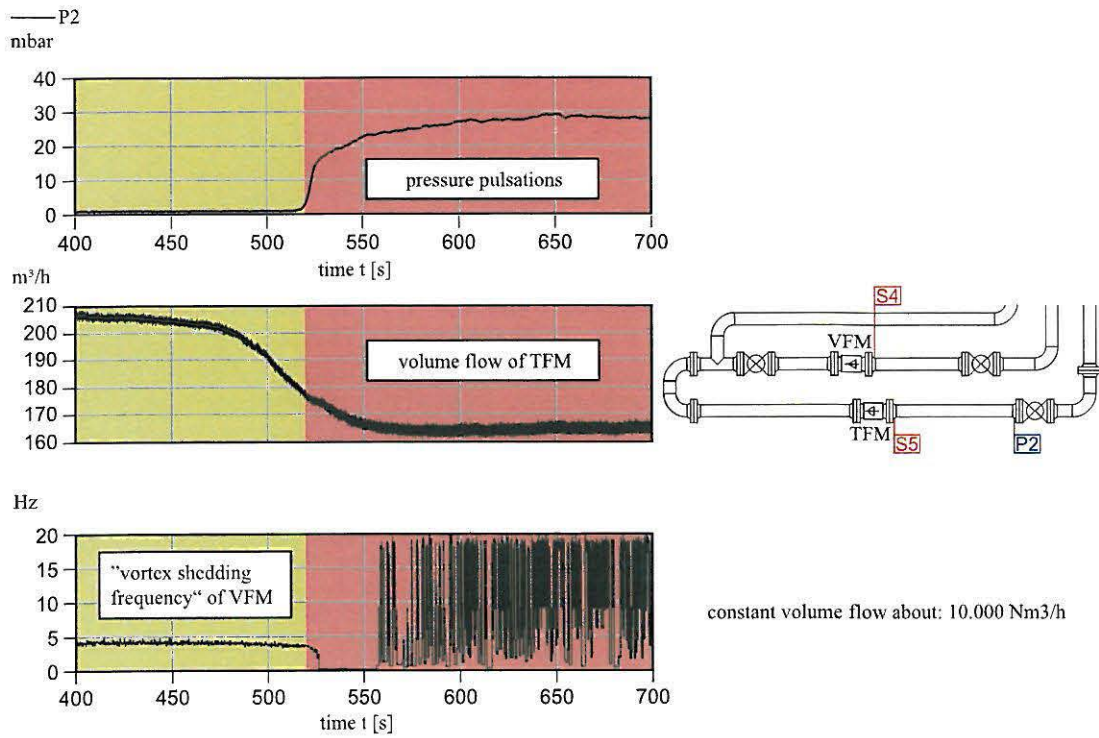


Fig. 3. Pressure pulsations, indicated volume flow at the TFM and vortex shedding frequency of the VFM before and after suddenly activating the heat exchanger at 520 s.

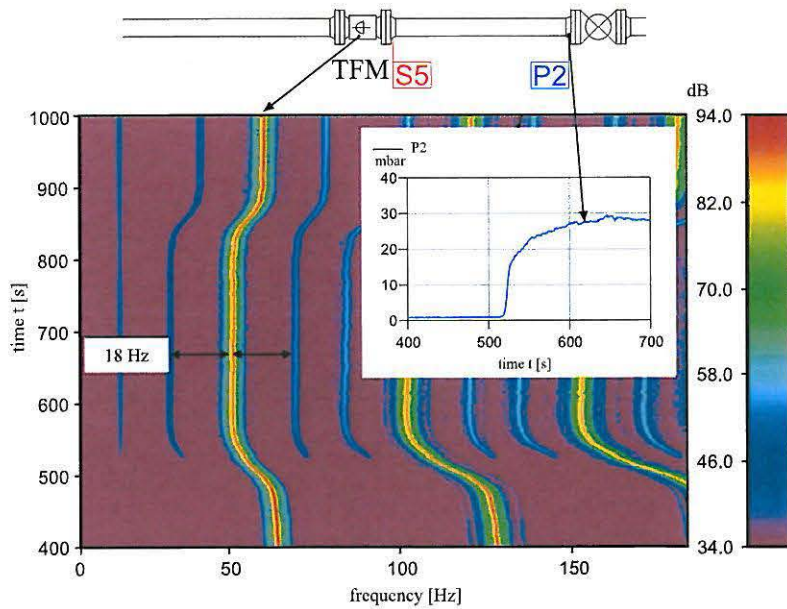


Fig. 4. Spectral analysis of the measured turbine wheel HF-signal before and after suddenly activating the heat exchanger at 520 s.

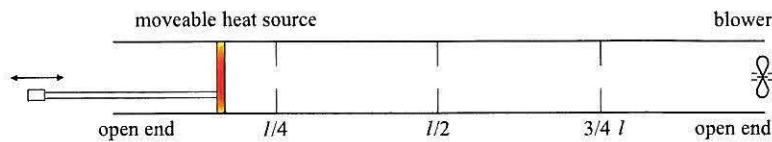


Fig. 5. Schematic layout of the Rijke tube.

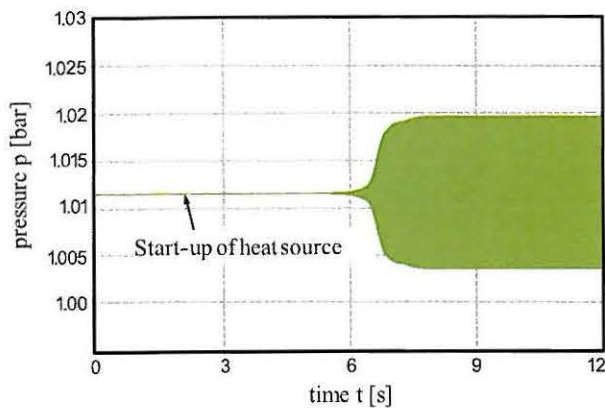


Fig. 6. Simulated time-dependent pressure pulsations at the position $l/4$ of the Rijke tube after starting the heat source at $t = 2$ s.

and hence the heat flow rate and the integrated heat input into the air are weakly fluctuating. The phase relation between a fluctuation of velocity and the heat input is predetermined for the one-dimensional simulation. As investigated by Putman and Dennis [3], the heat input lags the velocity fluctuation by a phase shift of $\pi/4$.

2.3. Results of the simulation calculations

A systematic variation of potential influencing factors is carried out in the simulation calculations. Due to the experience gained from measurements in gas pressure regulation and metering stations, the mean flow velocity in the pipe, the heat source temperature and the position of the heat source are varied. In order to receive further knowledge on the development of thermoacoustic vibrations, the impulse response of the system to a heat input impulse and the influence of the phase between velocity pulsations and heat input pulsations are also investigated. First, an example will illustrate the vibration behaviour of the investigated model of the Rijke tube before and after starting the heat source.

2.3.1. Pulsations before and after starting the heat source

With the simulation of the Rijke tube in the way described above, it is possible to simulate a thermoacoustically induced vibration. A precondition for the development of such a vibration is an already existing weak oscillation (e.g. due to surrounding noise) that can be amplified. For the simulation subsequently discussed, a weak oscillation was superposed to the average velocity—independent of the function of the heat source—whose intensity corresponds to human conversation with a pressure amplitude of $\hat{p}_0 = 52$ dB. The frequency of this initial disturbance is chosen to be the first natural frequency of the tube of 171.6 Hz at 20 °C (293 K). Therefore, even without the thermoacoustic amplification a weak standing wave is formed inside the Rijke tube (Fig. 6 before $t = 2$ s, too weak to be visible). The heat source is set at position $l/4$, put into operation at a certain turn-on instant and after this remains permanently activated.

As already described, a phase shift of $\pi/4$ is preset between the velocity fluctuation and the heat input fluctuation so that the pulsating heat input lags the velocity fluctuation. Due to the position of the heat source ($l/4$) and the predefined weak standing wave inside the tube this means that the pressure pulsation lags the heat input fluctuation by $\pi/4$ too. Accordingly—compared to the mean heat input value—more heat input will be given to the air in the moment of increased pressure (and vice versa) and therefore an initial exponential vibration growth is to be seen with a time lag to the turn-on instant. Afterwards, the vibration amplitude converges towards a fixed value where the pulsation excitation and the dissipation are at equilibrium. Exactly the

same principal behaviour (time lag, exponential growth, fixed final amplitude) was observed during the field investigations in gas pressure regulating and metering stations.

2.3.2. System response to a heat input pulse

Based on the Rayleigh criterion, two extreme cases for heat input limited in time were simulated. In one case, the singular heat input pulse is added at the moment of highest pressure, in the other case at the moment of lowest pressure. According to the Rayleigh criterion, maximal amplification or attenuation is expected.

Prior to the heat input pulse due to the weak superposed pulsation in both diagrams a standing wave in the tube can be seen. Accordingly at position $l/4$ (Fig. 7) the pressure pulsation lags the velocity pulsation by $\pi/2$. The triggered heat input pulse initiates a disturbance which, from the point of heat input, spreads into both directions with the speed of sound. After a time interval Δt_1 the reflected pulse of the close-by acoustically open tube end is clearly visible. The pulse after Δt_2 is triggered by the pulse reflected by the other acoustically open end of the tube. It is obvious that heat input at the moment of the highest pressure (right picture) results in an amplification of the pressure and velocity amplitudes and thus in an amplification of the initial pulsation. A similar system response with the same initial absolute values can be noticed in the case where the heat input pulse is activated at the moment of the lowest pressure (left picture). In this case the two reflected pulses result in a dampening of the initial pulsation. Thus the thermoacoustic effect is strongly dependent on the phase shift between the heat input fluctuation and the pressure fluctuation. Moreover, the mentioned phase shift between the velocity and pressure fluctuations of $\pi/2$ due to the weak standing wave inside the tube supports the build-up of the oscillation, because the heat input fluctuation usually lags the velocity pulsation by a phase shift of about $\pi/4$.

2.3.3. Influence of the phase shift between the velocity and heat input fluctuations

Following the examination of the pulse excitation, the influence of the predefined phase shift between the velocity pulsation and the heat input pulsation is systematically varied from 0 to π , with the heat input fluctuation generally lagging the velocity fluctuation. A sinusoidal dependence between the phase difference and the resulting pulsation amplification \hat{p} —related to the amplitude of the excitation \hat{p}_0 —is to be noticed, which shows a maximum at a phase difference close to $\pi/2$ (see Fig. 8). In this case, the heat input is in phase with the pressure pulsation. In the ranges of 0 to $\pi/12$ and $11/12\pi$ to π , the influence of the damping parameter prevails and the initial excitation is damped with an amplitude ratio of less than one. The standardised illustration of the integrated Rayleigh integral for sinusoidal functions of pressure pulsation p' and heat input fluctuation q' in the case of a fixed phase shift of $\pi/2$ between the velocity pulsation c' and p' (p' lagging c') shows a comparable amplification characteristic. Therefore it can be assumed that, with a higher value of the Rayleigh integral, the energy input into the acoustic wave is encouraged.

Thus, the simulation of the Rijke tube confirms the theoretical dependency of the phase difference between velocity pulsation and heat input pulsation on the amplification of an initial disturbance. Moreover, the Rayleigh integral may be used as a criterion to analyse the expected amount of energy input into the initial disturbance.

2.3.4. Influence of the mean flow velocity

Fig. 9 shows the dependence of the pulsation amplification on the time-averaged Reynolds number. This Reynolds number is

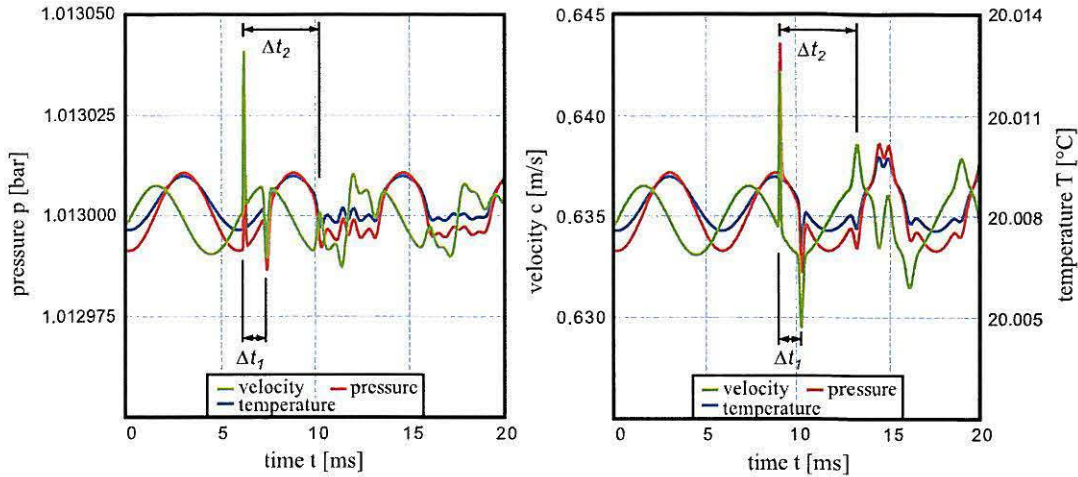


Fig. 7. Simulated system response to a single heat input pulse at $l/4$ at the moment of maximal expansion (rarefaction) (left) and compression (condensation) (right).

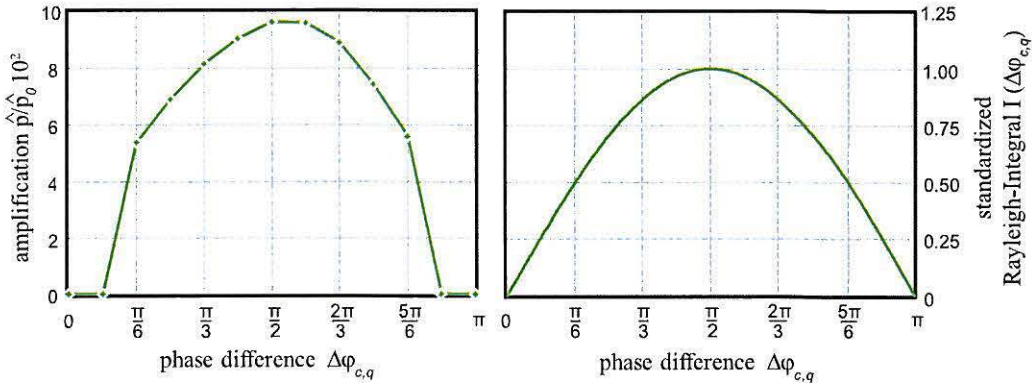


Fig. 8. Simulated standardised amplification of pressure pulsations depending on the phase shift between velocity pulsation and heat input fluctuation (left) and integrated Rayleigh-integral for sinusoidal functions of pressure and heat input pulsations depending on the phase shift between the pressure and velocity pulsations.

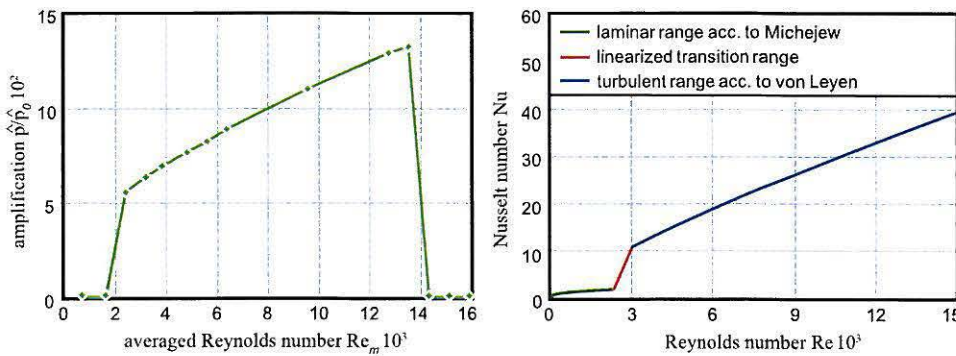


Fig. 9. Influence of the mean flow velocity on the amplification of pulsation inside the Rijke tube (left) and Nusselt number above the averaged Reynolds number (right).

directly proportional to the applied mean flow velocity inside the Rijke tube.

Up to a Reynolds number of about 2000 no amplification is observed. Above this Reynolds number a sudden strong amplification occurs. The amplification increases with increasing mean flow velocity up to a Reynolds number of about 14 000. At higher Reynolds numbers the amplification suddenly disappears again.

The heat transfer from the heat source to the air depends on the Nusselt number. This, in turn, depends on the Reynolds number calculated at the heat source in dependence on time. In the case of a pulsating flow velocity due to any initial disturbance, the Nusselt number and thus the heat flow and heat input are pulsating too.

For a predefined initial amplitude of the flow velocity pulsation the resulting amplitude of heat flow pulsation and consequently the amplitude of heat input is dependent on the derivative of the Nusselt number with respect to the Reynolds number. In the case of a small derivative the amplitude of heat input pulsation and hence the initial thermoacoustic excitation is weak.

The chosen equation for Nusselt numbers in the range of laminar flows does have a small gradient. Therefore the wall friction and throttling at the open ends of the Rijke tube prevail over the weak excitation of the initial superposed disturbance. Accordingly for Reynolds numbers below 2000 no amplification occurs.

Once the initial thermoacoustic excitation outbalances the dissipation the initial weak pulsation will be amplified. The resulting final amplification depends on two limiting factors. On the one hand with increasing pressure pulsations the velocity pulsations are increasing too. Therefore the time-dependent friction and throttling losses are enlarged. On the other hand in almost all amplified cases the numerically calculated final flow velocity pulsation amplitude is higher than the averaged flow velocity. Hence the flow velocity is temporarily negative. Because the time-dependent heat flow is a function of the absolute value of the time-dependent flow velocity a negative flow velocity corresponds to an increasing heat flow. From this it follows that there is a heat input into the air at the moment of reduced pressure. A partly negative flow velocity therefore reduces the thermoacoustic excitation. Both mechanisms cause the resulting amplification factor.

With increasing averaged Reynolds number the mean flow velocity is enlarged. Due to this temporarily negative flow velocities will occur only in the case of increased amplification factors. Therefore with increasing averaged Reynolds number the resulting amplification factor is enlarged. At the same time the dissipative induced attenuation increases with increasing averaged Reynolds number and with increasing amplification factors. In consequence the slope of the amplification is decreasing with increasing averaged Reynolds number.

At a certain value of averaged Reynolds number the amplification suddenly disappears. In this case the increased losses prevail over the initial thermoacoustic excitation of the superposed weak disturbance. The dissipation loss is increased due to the higher mean flow velocity. At the same time the initial thermoacoustic excitation is reduced due to the decreasing gradient of the Nusselt number equation used. Related to the model used for simulation the amplification disappears at averaged Reynolds numbers above 14 000 (flow velocity above 3.5 m/s). In general this value is not a physical constant. Among other influencing factors (e.g. the heat transfer model used, the phase shift between heat input fluctuations and velocity pulsations, the position of the heat source), this value strongly depends on the existing fluid mechanical power loss within the investigated system.

Compared to the analysed vibration problems at various gas pressure regulation and metering stations in principle a similar behaviour was observed. Above a certain volume flow rate the vibrations suddenly vanish. Concerning the introduced natural gas metering station (see Fig. 1) the vibrations disappeared at flow rates above 14 000 N m³/h. The corresponding Reynolds number in relation to the relevant diameter of 0.02 m (inner diameter of one tube of the tube bundle heat exchanger) is about 50 000 at a flow velocity of 1 m/s.

2.3.5. Influence of the heat source temperature

According to Fig. 10, an increase of the heat source temperature results in an increase of the pulsation amplification factor. Below a heat source temperature of 275 °C no amplification is observed.

The intensity of the initial velocity pulsation and hence the initial fluctuation of the Nusselt number is fixed. Independent hereof the amplitude of heat input fluctuation is increased in the case where the heat source temperature is raised. At low temperatures (below 275 °C) the dissipation prevails over the weak thermoacoustic excitation of the initial superposed pulsation. Calculations show that, assuming reduced loss coefficients, an amplification of the superposed initial disturbance occurs even at lower heat source temperatures. Once the initial thermoacoustic excitation dominates the friction losses, the initial pulsation is amplified until a new balance between dissipation and excitation is achieved. With increasing temperature of the heat source this balance is obtained at higher amplification factors.

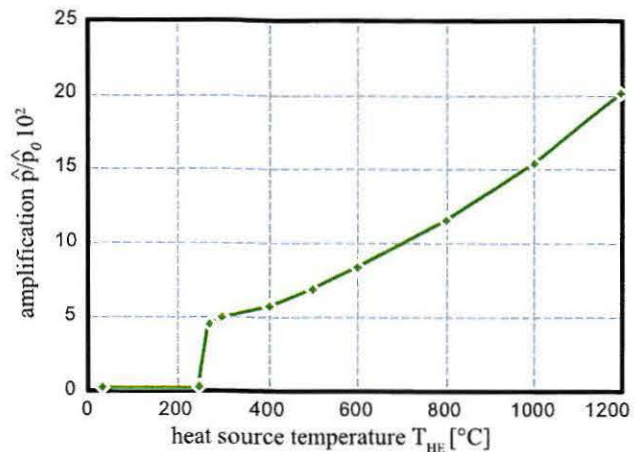


Fig. 10. Simulated standardised amplification of pressure pulsation inside a Rijke tube dependent on the heat source temperature.

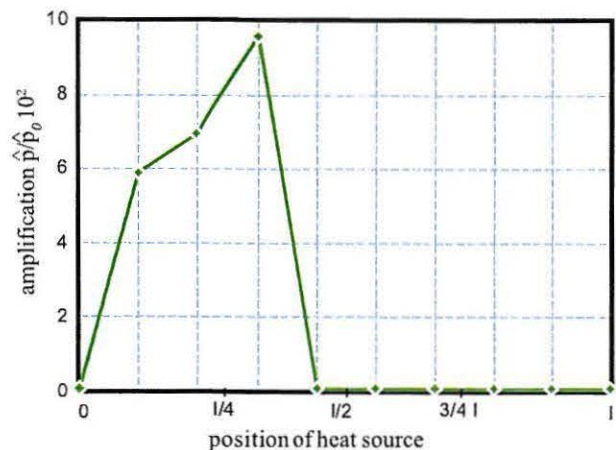


Fig. 11. Simulated standardised amplification of pressure pulsation inside a Rijke tube dependent on the heat source position.

2.3.6. Position of the heat source

The position of the heat source has a decisive influence on the amplification or attenuation of a superposed disturbance. Fig. 11 demonstrates that the initial superposed pulsation is amplified if the heat source is located in the left part of the Rijke tube (averaged flow from left to right). In the right part of the tube, attenuation takes place, because at this side the velocity pulsation lags the pressure pulsation by $\pi/2$. In combination with the predefined phase shift of $\pi/4$ between the velocity pulsation and the heat input fluctuation the Rayleigh index at the right side of the Rijke tube is therefore negative.

Compared to the Rayleigh integral along the whole Rijke tube, the analytically expected maximum of the amplification at $l/4$ is slightly shifted to the centre of the tube. The reason for this seems to be a shift of the acoustic natural frequency of the tube due to the heat input and the related local increase in the speed of sound.

3. Problem-solving approaches to prevent thermoacoustically induced vibrations in gas pressure regulation and metering stations

The analysed physical dependencies of the Rijke tube simulations may be used in order to design measures to avoid thermoacoustically induced vibration problems in gas pressure regulation and metering stations. The initial thermoacoustic excitation energy, the position of the heat exchanger and the dissipation loss

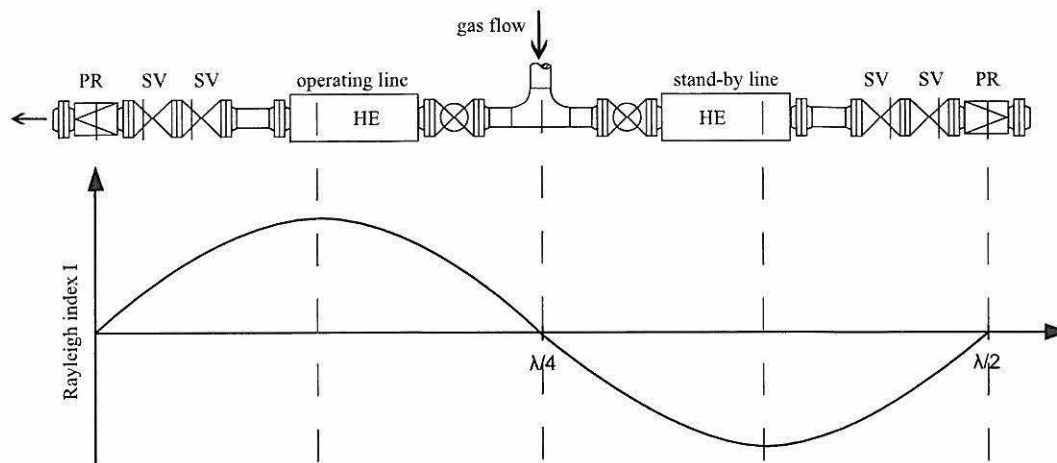


Fig. 12. Rayleigh index along the pipe calculated for the studied natural gas pressure regulation and metering station (right side closed).

turned out to be decisive parameters for the avoidance of thermoacoustically induced vibrations. Moreover, it is appropriate to transfer the calculation method and collateral conditions (e.g. predefined phase shift, heat transfer model) to the simulation of entire gas pressure regulation and metering stations. In particular, when new stations with changing operating conditions are designed, vibrations and vibration-induced disturbances of flow meters in the station therefore can be precalculated and avoided in the further planning process.

3.1. Thermoacoustic excitation energy

In particular, in stations where the heat exchanger temperature is not lowered or adjusted at low volume flows, the development of thermoacoustic vibrations may be encouraged. It is recommended to reduce the temperature difference between the heat exchanger and the gas in the case of reduced volume flows. In stations where control is not provided, a possible switch-off of the heat exchanger should be considered at low flow rates.

Besides, it is advisable to use control valves with reduced noise emission levels, e.g. due to specially designed control valve cages. Accordingly the initial flow velocity fluctuation and hence the initial thermoacoustic excitation is reduced.

3.2. Position of the heat exchanger

For a given station, the quantitative course of the Rayleigh index along the pipe can be calculated in dependence on the geometrical dimensions and the first natural pressure pulsation mode shape. Fig. 12 shows the control lines of the station presented in Fig. 1 in a simplified horizontal arrangement as well as the Rayleigh index calculated for the station. It turns out that the heat exchanger in the operating line is in the range of the maximum of the Rayleigh index and thus encourages the development of thermoacoustically induced vibration.

This correlation can be taken into account when a new station is planned. Vibration excitation can be avoided, e.g. by positioning the heat exchanger more closely to the T-piece or into the feed line. Moreover, regarding existing stations there is the possibility to equip a potential valve at the inlet of the stand-by line with a motor drive and to close it if the line is out of operation. The consequence is that the acoustic length of the pipe is reduced, which results in a shift of the maximum of the Rayleigh index towards the pressure regulating valve. Thus, the thermoacoustic excitation at least is reduced and the amplification of a given disturbance (e.g. due to the flow through the pressure regulation valve) may be completely avoided.

3.3. Dissipation

The simulation results have shown that from a certain amount of damping in the system, amplification of an existing disturbance no longer occurs. Consequently, thermoacoustically induced vibration can be avoided or reduced by increased damping. For example, it is advisable, recommended to install apertures or specially designed pulsation damping plates [7] in the area of high velocity fluctuations near the T-piece or at the inlet of the heat exchangers. Alternatively, vertically arranged tube bundle heat exchangers with U-bends can also be provided, which generally cause a higher pressure loss compared to horizontally arranged heat exchangers and thus contribute to the desired minimum damping. Another possibility to avoid thermoacoustically induced vibration is to avoid operation of the station below certain volume flows. The minimal permissible volume flow (Reynolds number), however, depends on the given damping inside the respective pipe section and cannot be universally given. From experience, flow velocities below 1–2 m/s inside the tubes of tube bundle heat exchangers should be avoided.

In order to eliminate the vibration problem at the mentioned station a pulsation damping plate [7] with a pressure drop of about 5 kPa at 10 000 N m³/h (line pressure of about 4.7 MPa at 10 °C) was designed and installed at the inlet flanges of the heat exchangers. After realization of this measure the thermoacoustic instability was gone and hence the vibration problem was solved.

4. Summary

A pipe vibration problem and the accompanying impacts on the measuring behaviour of the involved flow meters are presented using a surveyed gas pressure regulation and metering station as an example. The origin of the problem turns out to be a thermoacoustic instability in the area of two adjacent regulating lines with heat exchangers.

The Rijke tube experiment in principle enables the examination of thermoacoustically induced pulsations. In order to understand the physical dependencies a numerical simulation of the Rijke tube by means of the one-dimensional method of characteristics is carried out. The decisive influencing factors as well as the physical mechanism of action for the development of thermoacoustic pulsations are presented. The Rayleigh index as a criterion for the excitation of thermoacoustic oscillations is confirmed.

Based on the analysed physical dependencies approaches to the avoidance and/or reduction of thermoacoustically induced vibrations in gas pressure regulation and metering stations are given. The decisive influencing factors are the position of the heat

exchanger, the thermoacoustic excitation energy and the damping inside the gas pressure regulation and metering station.

An aim of future research is to avoid the development of thermoacoustic vibrations, e.g. by influencing the phase shift between the velocity and heat input fluctuations. Moreover, the thermoacoustic effect may be systematically used to attenuate existing pulsations, e.g. in the field of positive displacement machines by applying electrically regulated heat input. For this purpose, apart from theoretical considerations also experimental investigations are planned.

Acknowledgements

We would like to thank RWE Rheinland Westfalen Netz AG, Essen, FRG for the financial support granted to carry out the simulation with the aim of understanding the physical mechanisms of

action of thermoacoustic vibrations and to develop possible measures for the avoidance of such vibrations.

References

- [1] Sarpotdar S, Ananthkrishnan N, Sharma SD. The Rijke tube—a thermoacoustic device. *Resonance—Journal of Science Education* 2003;8:59–71.
- [2] Rayleigh Lord. The explanation of certain acoustic phenomena. *Natural* 1878; 18:319–21.
- [3] Putnam A, Dennis W. Burner oscillations of the gauze-tone type. *Journal of the Acoustical Society of America* 1954;26(5):716–25.
- [4] Schacht W. Gasnetzsimulation mit Hilfe des Charakteristikenverfahrens. *GWF-Gas-Erdgas* 2001;5:356–67.
- [5] Kentfield JAC. *Nonsteady, one-dimensional, internal, compressible flows—theory and applications*. New York (Oxford): Oxford University Press; 1993.
- [6] Kramer C, Mühlbauer A. *Praxishandbuch Thermoprozess-Technik*. Essen: Vulkan-Verlag GmbH; 2002.
- [7] Kötter Erwin. Dämpferplatte für den Einbau in Rohrleitungen. Patent no. DE19538178C1. 1997.